SUPPORTING INFORMATION

Large Current Driven Domain Wall Mobility and Gate Tuning of Coercivity in Ferrimagnetic Mn4N Thin Films

Toshiki Gushi[1,2], Matic Jovičević Klug[3,÷], Jose Peña Garcia[3], Sambit Ghosh[2], Jean-Philippe Attané[2], Hanako Okuno[4], Olivier Fruchart[2], Jan Vogel[3], Takashi Suemasu[1], Stefania Pizzini*[,3], Laurent Vila[†,2]

1. Institute of Applied Physics, Graduate School of Pure and Applied Sciences, University of Tsukuba, Tsukuba, Ibaraki 305-8573, Japan

2. Université Grenoble Alpes, CEA, CNRS, Grenoble INP, SPINTEC, F-38000 Grenoble, France

3. Université Grenoble Alpes, CNRS, Institut Néel, F-38042 Grenoble, France

4. Université Grenoble Alpes, CEA, IRIG, MEM, F-38000 Grenoble, France

*stefania.pizzini@neel.cnrs.fr

† Laurent.vila@cea.fr

÷Permanent address : Kiel University, Institute for Materials Science, Kaiserstraße 2, 24143 Kiel, Germany

Absence of Spin Orbit Torques

Domain Walls (DWs) having a chiral Néel structure stabilized by interfacial Dzyaloshinskii-Moriya interaction (DMI) can be driven by Spin-Orbit Torques (SOTs), arising from the Spin Hall Effect or from Rashba effects [1]. In order to exclude the contribution of SOTs to the DW dynamics in our system, we have carried out measurements aiming at establishing the nature of the DW structure. The domain wall dynamics was driven by an out-of-plane magnetic field, in the presence of a continuous longitudinal in plane field B_X. The domain wall velocity in the direction of the in-plane field depends on the nature of the internal DW structure. On one hand, in the case of Bloch walls, the DW speed increases as a function of B_X, and is the same for fields of opposite signs (*i.e.*, the speed vs. B_X curve is symmetric). On the other hand, the presence of DMI induces an asymmetry of the speed vs. B_X curve, with a minimum speed when the B_X field compensates the DMI field [2,3].

Examples of DW displacements in the absence and in the presence of an in-plane magnetic field of 400 mT are shown in Figure S1 (a,b). The white contrast in the Kerr images represents the displacement

of the DW during the field pulse. This displacement is isotropic in the presence of the in-plane field, which indicates the absence of DMI. The domain wall speed vs. Bx curve is shown in Figure S1 (c).

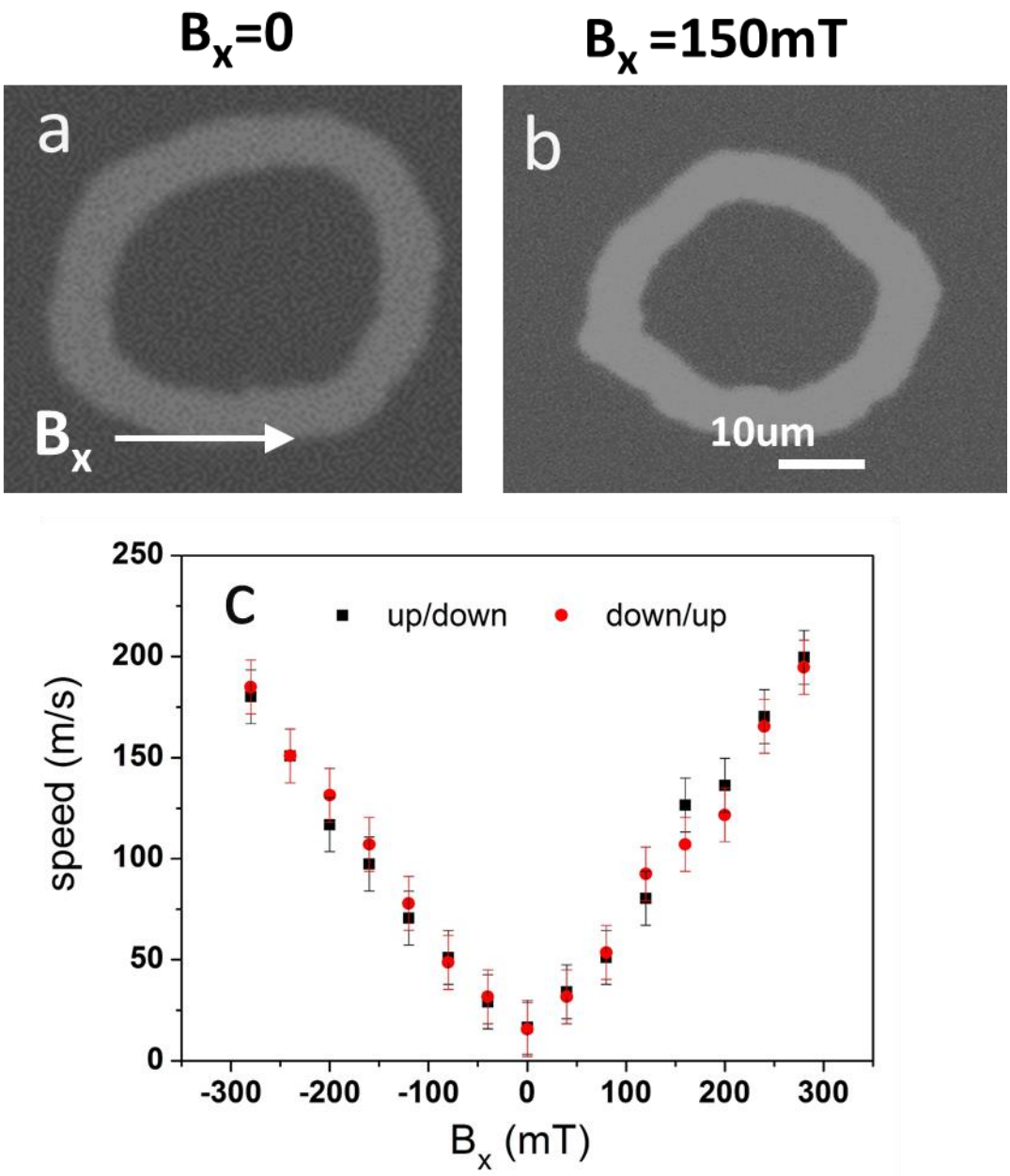

Figure S1. (a,b): Differential Kerr images showing the displacement of domain walls driven by an out-of-plane magnetic field pulse, of around 400mT and 30ns (white contrast) in the absence (a) and in the presence (b) of an in-plane continuous magnetic field B_X. (c): domain wall speed driven by B_Z= 320 mT perpendicular field pulses, as a function of the in-plane field amplitude B_X, for an up/down and a down/up domain wall. The symmetric curve confirms the presence of achiral domain walls.

Field and current driven domain wall dynamics

Magnetisation dynamics in ferromagnetic materials is governed by the Landau-Lifshitz-Gilbert equation, with additional terms added to account for other interactions such as the STT. Following the description proposed by Thiaville et al. [4], the magnetisation dynamics is given by:

$$\frac{\partial \boldsymbol{m}}{\partial t} = \gamma_0 \boldsymbol{H_{eff}} \times \boldsymbol{m} + \alpha \boldsymbol{m} \times \frac{\partial \boldsymbol{m}}{\partial t} - (\boldsymbol{u} \cdot \boldsymbol{\nabla})\boldsymbol{m} + \beta \boldsymbol{m} \times [(\boldsymbol{u} \cdot \boldsymbol{\nabla})\boldsymbol{m}] , \qquad (1)$$

where $\boldsymbol{m}$ is the unit vector along the local magnetisation, $\gamma_0 = \gamma\mu_0$ where γ is the gyromagnetic ratio and μ_0 the vacuum permeability, $\boldsymbol{H_{eff}}$ is the micromagnetic effective field, and α is the Gilbert damping constant. The spin-drift velocity $\boldsymbol{u}$ is parallel to the electron flow direction, with $\boldsymbol{u} = \frac{g\mu_B}{2eM_s} P$ where $g \approx 2$ is the free electron's Landé factor, μ_B the Bohr magneton, e the electron charge, P the current polarisation factor and M_s the spontaneous magnetisation. Finally, β is the non-adiabatic term, representing a second-order term of the STT.

Let us review now the DW dynamics features under an applied magnetic field and spin-polarized current using the 1D model. To describe the DW motion in the 1D model, two collective coordinates are chosen: the DW centre, q, and the tilt angle of the DW magnetisation out of the DW plane, φ. The DW profile is described by the following ansatz:

$$\theta(x,t) = 2 \arctan \exp\left(\frac{x - q(t)}{\Delta}\right), \qquad (2a)$$

$$\phi(x,t) = \varphi(t) , \qquad (2b)$$

Where $\boldsymbol{m} = (\sin\theta\cos\phi\,, \sin\theta\sin\phi\,, \cos\theta)$. Using a Lagrangian approach [5,6] we can find the equations of motion under current (applied along +x) and magnetic field applied along the easy-axis z:

$$\frac{1}{\Delta}\dot{q} - \alpha\dot{\varphi} = \frac{u}{\Delta} + \frac{\mu_0\gamma H_D}{2}\sin 2\phi, \qquad (3a)$$

$$\dot{\varphi} + \frac{\alpha}{\Delta}\dot{q} \quad = \beta\frac{u}{\Delta} + \mu_0\gamma H_{app}, \qquad (3b)$$

Here, $\Delta(\varphi) = \sqrt{\frac{A}{\mathrm{K_u} + \mathrm{K_D}(\varphi)}}$ is the DW width, where A is the exchange stiffness, K_u the uniaxial anisotropy, $K_D = \frac{\mu_0 M_S^2}{2}\left(N_x \sin^2\varphi + N_y \cos^2\varphi - N_z\right)$ (N_i being the demagnetizing coefficients), and $H_D = \frac{2K_D}{\mu_0 M_s}$ is the DW demagnetizing field [4].

When a DW is driven by a magnetic field, the DW moves in the steady regime with a constant value of φ up to a field called the Walker field (H_W). Above H_W, the DW moves by transforming continuously, *i.e.*, $\dot{\varphi} \neq 0$ (from transverse to vortex DW for in-plane systems and from Bloch to Néel DW in out-of-plane systems). This continuous transformation results in a drop of the velocity until it reaches a second linear v vs. H regime, with reduced mobility.

When the DW is driven by a spin polarized current, in the adiabatic limit ($\beta = 0$) the DW moves continuously only when it can start precessing and align with the incoming spin polarisation. This occurs above a threshold critical current density J_c:

$$J_c = \frac{2e}{\hbar P}\Delta(\varphi)K_D, \qquad (4)$$

Through the dependence on K_D, J_c depends on the value of the spontaneous magnetisation and on the geometry of the film strip [8]. In systems with in-plane magnetisation, the transverse anisotropy constant is given by $\mathrm{K_D} = \left|\mathrm{K_z} - \mathrm{K_y}\right| \approx |\mathrm{K_z}| = \frac{1}{2}\mu_0 \mathrm{M_s^2} - \mathrm{K_u}$. On the other hand, in thin films with perpendicular magnetisation, the transverse anisotropy constant, which is related to the energy difference between a Bloch and a Néel DW, is given by $\mathrm{K_D} = \left|\mathrm{K_x} - \mathrm{K_y}\right|$. For a thin strip of thickness t and width w, the DW can be modeled as an ellipse and the demagnetizing factors can be approximated as $\mathrm{K_x} \approx \frac{1}{2}\mu_0 \mathrm{M_s^2}\left(\frac{\mathrm{t}}{\mathrm{t}+\pi\Delta}\right)$, $\mathrm{K_y} \approx \frac{1}{2}\mu_0 \mathrm{M_s^2}\left(\frac{\mathrm{t}}{\mathrm{t}+\mathrm{w}}\right)$ [7]. Using the experimental M_s for a 1 µm wide and 10 nm thick Mn_4N strip like in our experiments, we obtain $\mathrm{K_D}$ ≈1.1 x 10^3 J/m^3. This value is much lower than that obtained for a permalloy strip with the same geometry ($\mathrm{K_D}$ ≈0.5 x 10^6 J/m^3). From Equation 4, using A=10pJ/m in the expression of the domain wall parameter, the critical current density for Mn_4N is of the order of 1.9 x 10^{10} A/m^2 while the one for permalloy is at least a factor 100 larger. Note that the exchange stiffness (A) of Mn_4N films has not been measured but it has been evaluated by scaling its Curie temperature to that of other nitrate compounds. Using A values between 4pJ/m and 30pJ/m (extreme values found for transition metal alloys) we obtain J_c between 1.35 and 3.25 x 10^{10} A/m^2. The measured depinning current density can be extrapolated to be around 2-3 x 10^{11} A/m^2 (see Figure 3) which is, for each value of A, much larger than the theoretical critical current corresponding to intrinsic pinning.

In the adiabatic limit, for current densities above J_C, the DW starts precessing and moves at a velocity given by:

$$\boldsymbol{v_{precession}} = \frac{1}{1+\alpha^2}\sqrt{\boldsymbol{u^2} - \boldsymbol{u_c^2}} \quad (5)$$

where $\mathbf{u_c}$ is the spin-drift velocity at the critical current density. When the critical current density is very small (as it is the case for systems with PMA), the latter expression can be approximated:

$$\boldsymbol{v_{precession}} \approx \frac{1}{1+\alpha^2}|\boldsymbol{u}| = \frac{1}{1+\alpha^2}\frac{g\mu_B}{2eM_s}P\boldsymbol{J} \quad (6)$$

This expression then shows that the DW mobility in the precessional regime is proportional to the ratio between the spin polarisation and the spontaneous magnetization. Large mobilities are then expected for large polarisation and small M_S.

In order to confirm the different features predicted by the 1D model, we have performed micromagnetic simulations with the finite-difference software MuMax3 [9] in the pure adiabatic limit.

In order to limit the calculation time, the strip width was fixed to 120nm and its thickness to 1nm. We have compared the case of an in-plane magnetized system ($M_s = 1.4 \cdot 10^6\ A/m$, $K_u = 9.75 \cdot 10^5\ J/m$^3 and Q=0.79) with an out-of plane system ($M_s = 1.4 \cdot 10^6\ A/m$, $K_u = 1.95 \cdot 10^6\ J/m$^3 and $\mathrm{Q} = 1.51$), where $Q = \frac{2K_u}{\mu_0 M_s^2}$ is the so-called quality factor. The obtained current-driven DW velocities are shown in Figure S2. For Q=1.51 an overall agreement is obtained with the 1D model: the critical current density is of the order of $10\ u \approx 2 \cdot 10^{10} A/m^2$ so that the DWs start moving linearly starting from very low current densities. Slight differences with respect to the 1D model appear for very low values of u (cf. inset of Fig. S2): the DW moves discontinuously because of extrinsic effects,

but it can nevertheless be displaced over some distance by the application of a current larger than J_c. Moreover, for high values of J, some deviations from the linear regime are observed. These deviations are associated to the DW asymmetry [10,11] and to the constraints on the magnetisation dynamics introduced by the use of the ansatz in the 1D model. The 1D model considers only 2 collective coordinates (q, φ), whereas in a 2D extension of this model, the asymmetry is taken into account by considering an extra collective variable, χ [11].

When $Q < 1$, for in-plane magnetized systems, the high dipolar cost for bringing the magnetisation out-of-the-plane and into precession traduces into a high critical current (about $300\,u \approx 8 \cdot 10^{12} A/m^2$) as expected from Equation 4. The linear regime of motion is then obtained for much larger current densities.

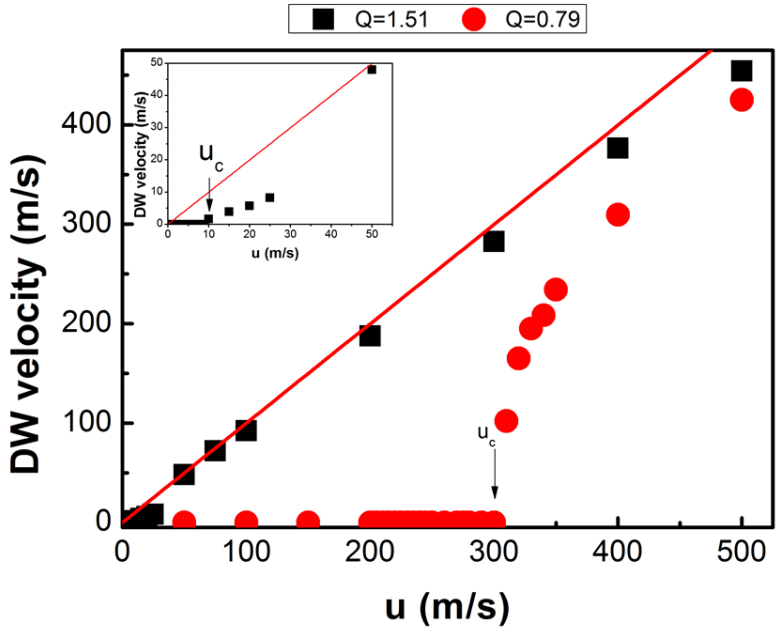

Figure S2. Micromagnetic simulations showing the DW velocity as a function of the spin-polarized current density, for two different values of Q: $Q = 1.51$ (black squares) and $Q = 0.79$ (red dots). The red solid lines represents the 1D model velocity (Eq. 6). The inset shows the details for small values of the spin-drift velocity.

Influence of the non-adiabatic torque and of the damping parameter on the current-induced DW motion

Up to now we have neglected the effect of the non-adiabatic torque in the dynamics of DWs in PMA systems. While this term had to be considered to explain the DW motion observed experimentally in in-plane magnetized systems like permalloy strips below the intrinsic Jc, we have shown that the large DW velocities observed in our Mn_4N stripes for low current densities can be explained by the adiabatic term alone. It has been shown analytically that the non-adiabatic torque results in a steady regime motion with velocity $v = \frac{\beta}{\alpha} u$ below the critical current J_c. On the other hand, a term $\frac{a\beta}{1+a^2} u$ is added to the velocity in the precession regime [3]. However, since α is much smaller than 1 in Mn_4N (0.15 according to time-resolved Kerr measurements) and β is expected to be of the same order of

amplitude as α [12], the non-adiabatic term contribution should be negligible with respect to the adiabatic one.

In order justify our choice to neglect the non-adiabatic torque, we performed micromagnetic simulations considering two extreme cases: $\beta = 2.5\ \alpha$ and $= 0.5\ \alpha$, with $\alpha = 0.15$. The results are shown in Figure S3.

When the non-adiabatic torque is taken into account, the DW moves in the steady regime until it reaches the Walker spin-drift velocity:

$$u_W = u_c \cdot \frac{\alpha}{|\beta - \alpha|} \qquad (6)$$

as shown in Figure S3(a). Note that when the non-adiabatic torque is neglected, the Walker spin-drift velocity coincides with the critical spin-drift velocity. Beyond J_c, as described previously the DW starts moving linearly with J, in the precessional regime, and the DW mobility is practically independent from the value of β (Figure S3 (b)).

These results led us to conclude that the non-adiabatic torque is not necessary to explain the velocities obtained experimentally. Nevertheless, our experiments do not allow to exclude *a priori* the presence of the non-adiabatic term, because the regime where it expresses itself, below J_c, is hidden by the thermally activated regime.

The Gilbert damping plays a critical role in the DW motion. In order to evaluate the impact of the value of alpha to the DW mobility, we have carried out micromagnetic simulations for the case $\alpha = 0.03$ and $\alpha = 0.3$ (either much smaller or much larger than that determined experimentally, $\alpha = 0.15$) and compared the results with the 1D model. The latter is the typical Gilbert damping value obtained for nm-thick Co layers deposited on high spin-orbit Pt layers. The results are shown in Figure S4. The difference in velocity for the maximum current density considered here is only about 6%. The larger damping also results into a larger u_c but the difference is negligible (see inset of Figure S4).

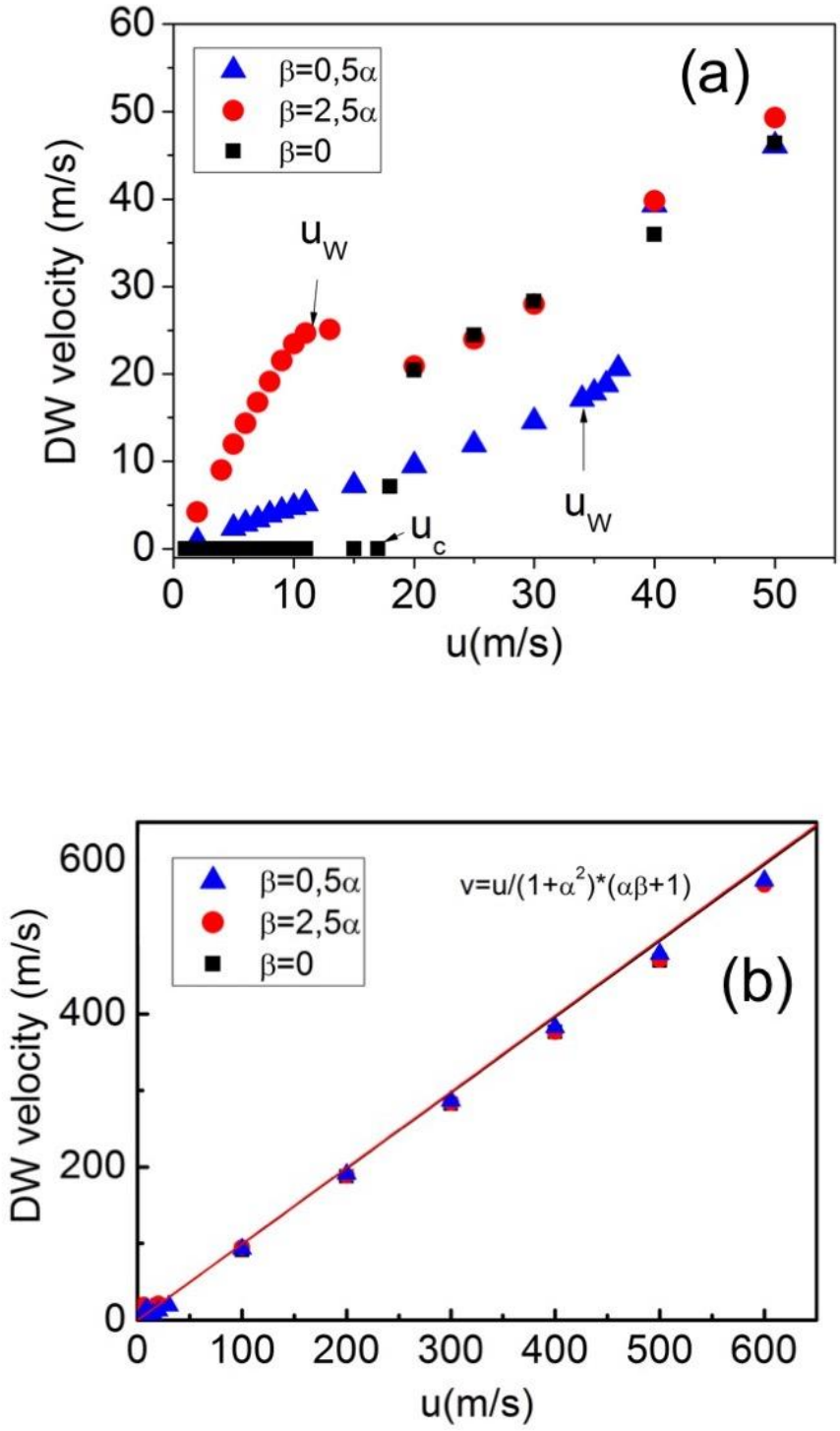

Figure S3. Results of micromagnetic simulations showing the DW velocity as a function of the spin-polarized current for different values of β: $\beta = 2.5\alpha$ (red circles), $\beta = 0.5\alpha$ (blue triangles) and $\beta = 0$ (black squares), for (a) low current and (b) large current densities. The red solid line represent the 1D model velocity (Eq. 5).

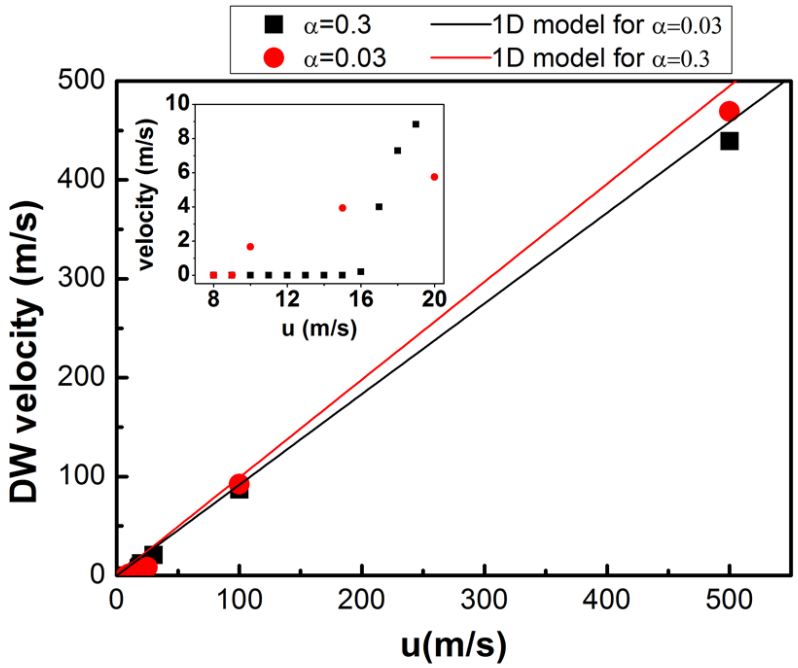

Figure S4. Results of micromagnetic simulations showing the DW velocity as a function of the spin-drift-velocity for two different values of α: $\alpha = 0.03$ (red circles), $\alpha = 0.3$ (black squares) . The solid lines represent the 1D model velocity (Eq. 5).

Damping and non-adiabatic torque: the particular case for which α=β

So far, we have divided the DW motion behaviour in two regimes: the steady regime below the Walker breakdown, and the precessional regime for currents above the Walker breakdown. Simulating the DW motion in the precessional regime, and modelling our system as a low-damping material (which implies that $v_{precession} \approx u$) has allowed us to reproduce the experimental DW velocities.

However, when the Gilbert damping and the non-adiabatic torque compensate each other, *i.e.*, in the hypothesis where $\alpha = \beta$, the 1D model predicts that the Walker spin-drift velocity becomes infinite (Eq.6). In this particular case, the DW moves in the steady regime at a velocity equal to the spin-drift velocity $v_{steady} = u$, whatever the applied current density. In order to confirm this result, we have simulated a PMA strip with $Q = 1.51$, and $\alpha = \beta = 0.03$. The results are shown in Figure S5 (a) where they are compared with the case $\beta = 0$. We can note that the velocities do not vary significantly between the two cases. On the other hand, the DW moves as expected in the precessional regime when $\beta = 0$, while it moves in the steady flow regime when $\alpha = \beta$. This is confirmed by the temporal evolution of the averaged x- and y- components of the DW magnetisation that are plotted in Figure S5 (b-c).

Note that an experimental evidence of a case where $\alpha = \beta$ has been reported [13,14]. Here, owing to the small difference between the DW velocity when the non-adiabatic and the damping torque are balanced or unbalanced, we cannot distinguish experimentally between the two cases.

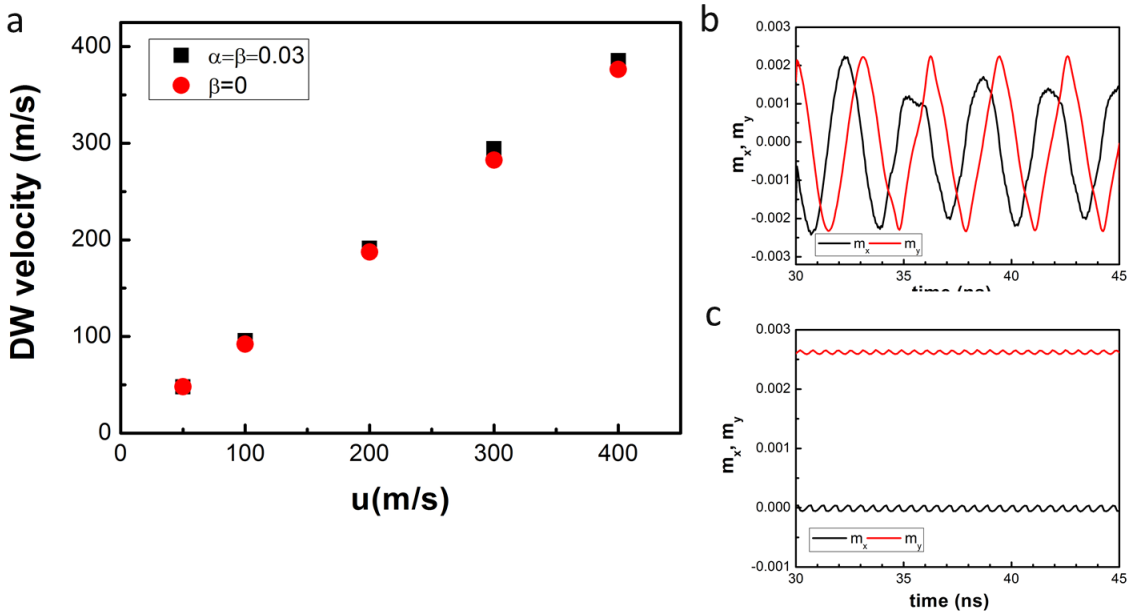

Figure S5. Results of micromagnetic simulations showing (a): the DW velocity as a function of the spin-drift velocity for $\beta = 0$ and $\beta = \alpha = 0.03$**.** (b,c): the temporal evolution of the averaged x- and y- DW magnetic components: $\beta = \alpha = 0.03$ (b) and $\beta = 0$ (c) for u=50.

Simulations details

We have performed micromagnetic simulations with the finite-difference software MuMax3 [9]. Zero-temperature simulations were performed in a defect-free strip of 6000×120×10 nm^3 with a cell size of 2.5×2.5×10 nm^3. For the study of the influence of $Q = \frac{2K_u}{\mu_0 M_S^2}$ on the DW motion, we set M_S=1.4×10^6 A/m and we tuned K_U. For the simulations of the experiments we set M_S=7.1×10^4 A/m and K_U=0.16×10^6 J/m^3. The rest of magnetic parameters were: A=10 pJ/m, P=0.7, α=0.15, β=0.

In a first step, the DW configuration in equilibrium was found in the absence of a spin-polarized current. In a second step, a current was applied along the positive x-axis, inducing an adiabatic torque resulting into the DW motion. We set up a post-step function that makes the simulation box "follow" the DW. The DW velocity was calculated by fitting the DW position as a function of time, 25 ns after the current was switched on, to ensure that all transient effects are damped out.

Finally, the influence of the cell size, of the damping parameter, of the DW width, of the non-adiabatic torque, and of the geometry were also tested. It was concluded that in the precession regime, none of these parameters strongly affects the DW motion.

References:

1 Khvalkovskiy, A. V.; Zvezdin, K. A.; Gorbunov, Ya.V.; Cros, V.; Grollier, J.; Fert, A.; Zvezdin, A. K. High Domain Wall Velocities due to Spin Currents Perpendicular to the Plane. Phys. Rev. Lett. **2009**, 102, 067206.

2 Je, S.-G.; Kim, D.-H.; Yoo, S.-C.; Min, B.-C.; Lee, K.-J; Choe, S.-B. Asymmetric magnetic domain-wall motion by the Dzyaloshinskii-Moriya interaction. Phys. Rev. B 2012, 88, 1440.

3 Hrabec, A.; Porter, N. A.; Wells, A.; Benitez, M. J.; Burnell, G.; McVitie, S.; McGrouther, D.; Moore, T. A.; Marrows, C. H. Measuring and tailoring the Dzyaloshinskii-Moriya interaction in perpendicularly magnetized thin films. Phys. Rev. B 2014, 90, 020402.

4 Thiaville, A.; Nakatani, Y.; Miltat, J.; Suzuki, Y., Micromagnetic understanding of current-driven domain wall motion in patterned nanowires. *Europhysics Letters 2005*, *69*(6), 990.

5 Huber, A. Theorie der Domänenwände in geordneten Medien. Springer, 1974.

6 Nasseri, S. A.; Sarma, B.; Durin, G.; Serpico, C. Analytical Modelling of Magnetic DW Motion. *Physics Procedia 2015*, *75*, 974-985.

7 Mougin, A.; Cormier, M.; Adam, J. P.; Metaxas, P. J.; Ferré, J. Domain wall mobility, stability and Walker breakdown in magnetic nanowires. *Europhysics Letters 2007*, *78*(5), 57007.

8 Emori, S.; Beach, G. S. Enhanced current-induced domain wall motion by tuning perpendicular magnetic anisotropy. *Applied Physics Letters 2011*, *98*, 132508.

9 "The design and verification of mumax3", AIP Advances 2014, 4, 107133.

10 Vandermeulen, J.; Van de Wiele, B.; Vansteenkiste, A.; Van Waeyenberge, B.; Dupré, L. A collective coordinate approach to describe magnetic domain wall dynamics applied to nanowires with high perpendicular anisotropy. *Journal of Physics D: Applied Physics 2015*, *48*, 035001.

11 Boulle, O.; Rohart, S.; Buda-Prejbeanu, L. D.; Jué, E.; Miron, I. M.; Pizzini, S.; Vogel, J.; Gaudin, G.; Thiaville, A. Domain wall tilting in the presence of the Dzyaloshinskii-Moriya interaction in out-of-plane magnetized magnetic nanotracks. *Physical review letters 2013*, *111*, 217203.

12 Malinowski G.; Boulle O.; Klaui M. Current-induced domain wall motion in nanoscale ferromagnetic elements, Journal of Physics D: Applied Physics 2011, 44, 3840005.

13 Adam, J.P. ; Vernier, N. ; Ferré, J.; Thiaville, A.; Jeudy, V.; Lemaître, A.; Thevenard, L.; Faini, G. Non adiabatic spin-transfer torque in (Ga,Mn)As with perpendicular anisotropy, Phys. Rev. B 2009, 80, 193204.

14 Curiale, J.; Lemaître, A.; Ulysse, C.; Faini, G.; Jeudy, V. Spin Drift velocity, polarization and current-driven domain wall motion in (Ga,Mn)(As,P). Phys. Rev. Lett. 2012, 108, 076604.